ACS SENSORS

Subscriber access provided by Kaohsiung Medical University

Article

# A pH-resolved colorimetric biosensor for simultaneous multiple targets detection

Nan Hao, Jinwen Lu, Zhou Zhou, Rong Hua, and Kun Wang

*ACS Sens.*, **Just Accepted Manuscript** • DOI: 10.1021/acssensors.8b00717 • Publication Date (Web): 17 Sep 2018

**Downloaded from http://pubs.acs.org on September 18, 2018**

## Just Accepted

"Just Accepted" manuscripts have been peer-reviewed and accepted for publication. They are posted online prior to technical editing, formatting for publication and author proofing. The American Chemical Society provides "Just Accepted" as a service to the research community to expedite the dissemination of scientific material as soon as possible after acceptance. "Just Accepted" manuscripts appear in full in PDF format accompanied by an HTML abstract. "Just Accepted" manuscripts have been fully peer reviewed, but should not be considered the official version of record. They are citable by the Digital Object Identifier (DOI®). "Just Accepted" is an optional service offered to authors. Therefore, the "Just Accepted" Web site may not include all articles that will be published in the journal. After a manuscript is technically edited and formatted, it will be removed from the "Just Accepted" Web site and published as an ASAP article. Note that technical editing may introduce minor changes to the manuscript text and/or graphics which could affect content, and all legal disclaimers and ethical guidelines that apply to the journal pertain. ACS cannot be held responsible for errors or consequences arising from the use of information contained in these "Just Accepted" manuscripts.

ACS Publications

is published by the American Chemical Society. 1155 Sixteenth Street N.W., Washington, DC 20036

Published by American Chemical Society. Copyright © American Chemical Society. However, no copyright claim is made to original U.S. Government works, or works produced by employees of any Commonwealth realm Crown government in the course of their duties.

# A pH-resolved colorimetric biosensor for simultaneous multiple targets detection

Nan Hao[a], Jinwen Lu[a], Zhou Zhou[a], Rong Hua[a], Kun Wang[a,b] *

[a] Key Laboratory of Modern Agriculture Equipment and Technology, School of Chemistry and Chemical Engineering, Jiangsu University, Zhenjiang 212013, PR China

[b] Key Laboratory of Sensor Analysis of Tumor Marker, Ministry of Education, College of Chemistry and Molecular Engineering, Qingdao University of Science and Technology, Qingdao 266042, PR China

Tel.: +86 511 88791800; E-mail address: wangkun@ujs.edu.cn (K. Wang)

## Abstract

Colorimetric detection has been widely applied in daily life. However, on the other hand, the further development of colorimetric biosensors has been constrained by the lack of multiple detection capabilities. In this work, we proposed a pH-resolved colorimetric biosensor for the first time for the simultaneous detection of four targets, including ochratoxin A (OTA), aflatoxins B1 (AFB1), fumonisin B1 (FB1) and microcystin-LR (MC-LR). With allochroic dyes as the signal indicators, pH value was introduced as the new dimension to control the release of dyes. The concentrations of four targets can be obtained in order by adjusting the pH of the solution. Meanwhile, tedious and high-cost chemical modifications processes in the fabrications of biosensors were also avoided by the combination of DNA-directed self-assembly of graphene oxide and magnetic separation. This biosensor provided a simple, rapid, accurate and low-cost strategy for multiple targets detection.


**Keywords:** Colorimetric biosensor; Mycotoxin; Aptamer; Food safety; Multiplex detection

Due to the advantages of low-cost, portability and easy-operation, colorimetric detection has been widely applied in daily life for various kinds of targets detection, such as DNA,[1] proteins,[2] cells,[3] toxins,[4] heavy metal ions[5-6] . Compared with other analytical methods such as mass spectrumy[7] and chromatography,[8] colorimetric sensing does not require sophisticated instruments and the quantification of targets can be achieved by naked eyes, making it suitable for point of care testing or field testing. At present, most colorimetric sensors transform the detection events into apparent color changes through two approaches. One way is to utilize enzymes[9] or enzyme-like materials[10-12] that can catalyze chemical reactions with color changes. For example, horseradish peroxidase (HRP) could catalyze tetramethylbenzidine (TMB) for the generation of blue color in the presence of hydrogen peroxide ($H_2O_2$).[13-14] Another approach is based on the surface plasmon resonance of noble metal nanomaterials.[15] The presence of targets can induce the change of distances[16-17] or the dispersion status[18-19] of nanomaterials and cause the color variation.

Although many colorimetric biosensors have been designed according to above two principles, the current design is mainly based on a single color change, which seriously limits the multiplex detection application of colorimetric biosensors. Until now, there are few reports about colorimetric biosensor that can achieve multiplex detection.[20] Erickson's group used gold and silver nanoparticles together in one solution,[21] and two targets can respectively induce the aggregation of gold or silver nanoparticles. The corresponding color changed at 520 nm and 404 nm can be seen independently depending on the concentration of each target. Allochroic dyes can also be used as the signal indicators for the multicolor detection.[22] Therefore, the problem of multiplex detection can be partially solved by using multiple signal indicators with colors of different wavelengths. But the visible light area was a narrow band

in the electromagnetic spectrum (around 400-700 nm), so the coexistence of multi-colors would interfere with each other due to the spectra overlapping. On the other hand, the recognition capability of human eyes can't tell the ratios and concentrations of different colors when more than three colors are mixed together. Thus, this strategy is only feasible for two or three targets detection. Considering the potential of further utilizing wavelengths to distinguish colors is limited, it's natural to figure out a new dimension, such as time or electric potential,[23-24] as the control measure to make colors appear in order. In this situation, two signal indicators, even have the same colors, can be applied for dual targets detection because they will be separated in the new dimension.

Global contamination of food by mycotoxins has become a serious problem because they cause diseases to humans, animals and corps, and cause economic losses in human society.[25-26] Therefore, as a global issue, food safety is gaining more and more attention. In this work, with four allochroic dyes as the signal indicators, the pH value was introduced as the new dimension to overcome the mutual interference of dyes and a pH-resolved colorimetric biosensor was developed for simultaneous detection of ochratoxin A (OTA), aflatoxins B1 (AFB1), fumonisin B1 (FB1) and microcystin-LR (MC-LR) . The concentrations of four targets can be obtained in order by adjusting the pH of the solution. Meanwhile, tedious and high-cost chemical modifications processes in the fabrications of biosensors were also avoided by the combination of DNA-directed self-assembly of graphene oxide and magnetic separation.[27-28] This biosensor provided a novel strategy for multiple targets detection, which is simple, rapid, accurate and low-cost.

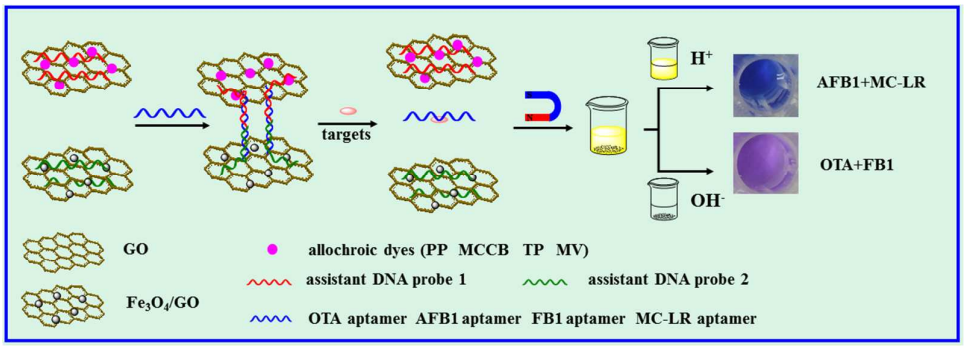


**Scheme 1.** Working principle of the colorimetric visual detection of OTA, AFB1, FB1, MC-LR. DNA probe 1 and probe 2 are partially complementary strands to the aptamer and hybridize simultaneously with the aptamer to form the GO assembly. The presence of targets would bind with aptamer and cause the dissociation of the assembly. After the biorecognition and magnetic separation, pH value was introduced as the new dimension to control the release order of dyes from the graphene to quantify targets.

## Experimental

### Reagents and Chemicals

Phosphate, phenolphthalein (PP), methyl violet (MV), thymolphthalein (TP), ferric chloride ($FeCl_3$), ferrous chloride ($FeSO_4 \cdot 7H_2O$) were purchased from Sinopharm Chemical Reagent Co. Ltd (China), Graphene oxide (GO) was purchased from Nanjing XFNANO Materials Tech Co. and malachite green carbinol base (MGCB) were purchased from Sigma-Aldrich. OTA, fumonisin B1 (FB1) and aflatoxins B1 (AFB1) were purchased from Sigma-Aldrich**.** Microcystin-LR (MC-LR) were obtained from J&K Chemical Ltd.(Shanghai). Semi-complementary OTA aptamer ($DNA_1$ and $DNA_2$) and OTA aptamer, Fluorescent dye labeled OTA aptamer (FOTA aptamer), semi-complementary AFB1 aptamer ($DNA_3$ and $DNA_4$) and AFB1 aptamer, semi-complementary FB1 aptamer ($DNA_5$ and $DNA_6$) and FB1 aptamer, semi-complementary MC-LR aptamer ($DNA_7$ and $DNA_8$) and MC-LR aptamer were obtained from Sangon Biotech Co., Ltd. (China) (Their sequences were shown in Table S1). Formulating phosphate buffered saline (PBS, $Na_2HPO_4$-$NaH_2PO_4$, 0.1 M)

in the laboratory; Doubly distilled water (18.2MΩ) was used throughout the experiment.

Apparatus

Atomic force microscopy (AFM) measurements were carried out using Bruker Innova Microscope instrument. Transmission electron microscopy (TEM) were performed on a JEOL 100 instrument (JEOL, Japan) at an accelerating voltage of 200 kV. Fluorescence spectra were recorded on a Hitachi F-4500 fluorescence spectra-photometer (Tokyo, Japan). UV–vis absorption spectra were characterized by spectrophotometer (UV-2450, Shimadzu, Japan). All the photos were taken with a Sony digital camera.

## Results and discussion

Experimental mechanism and verification

The principle of colorimetric biosensor for simultaneous detection of four targets (OTA, AFB1, FB1 and MC-LR) is shown in Scheme 1. The biosensor was composed of two GO platforms,[29] allochroic dyes and assistant DNA probe 1 absorbed GO (dyes-probe 1-GO) and assistant DNA probe 2 absorbed $Fe_3O_4$/GO (probe 2-$Fe_3O_4$/GO).[30] Allochroic dyes include phenolphthalein (PP), malachite green carbinol base (MGCB), thymolphthalein (TP) and methyl violet (MV) for four targets. And assistant DNA probes are partially complementary strands to the aptamer, which correspondingly changes for different targets and aptamers (Table S1). When the two GO platforms were mixed with aptamer in solution, assistant DNA probe 1 and probe 2 hybridized simultaneously with the aptamer and then a GO assembly was formed. The presence of targets would bind with aptamer and cause the dissociation of the assembly. In the consequent magnetic separation, with the concentration of targets increasing, more dyes-probe 1-GO would be left in the supernatant. Otherwise, they

would assemble with the $Fe_3O_4$/GO forming dye-GO-aptamer-$Fe_3O_4$/GO by aptamer binding and attracted into the precipitate by magnetic field. After the biorecognition and magnetic separation, pH value was introduced as the new dimension to control the release order of dyes from the graphene. When acidic water (AW) was added to the supernatant, the MGCB and MV molecules absorbed on GO surfaces were released because of the transformation from a neutral hydrophobic moiety to an hydrophilic moiety. [22]The color of the supernatant changed to a mixture of green (MGCB) and purple (MV). Due to the proportional relationship between the target and the dye, the color intensities of MGCB and MV represent the concentrations of AFB1 and MC-LR, respectively. When basic water (BW) was added to the precipitate, the PP and TP absorbed on GO surfaces were also released. The color of the precipitate changed to a mixture of pink (PP) and blue (TP). Then the concentrations of OTA and FB1 can be obtained respectively based on the inverse relationship between OTA and PP or FB1 and TP.

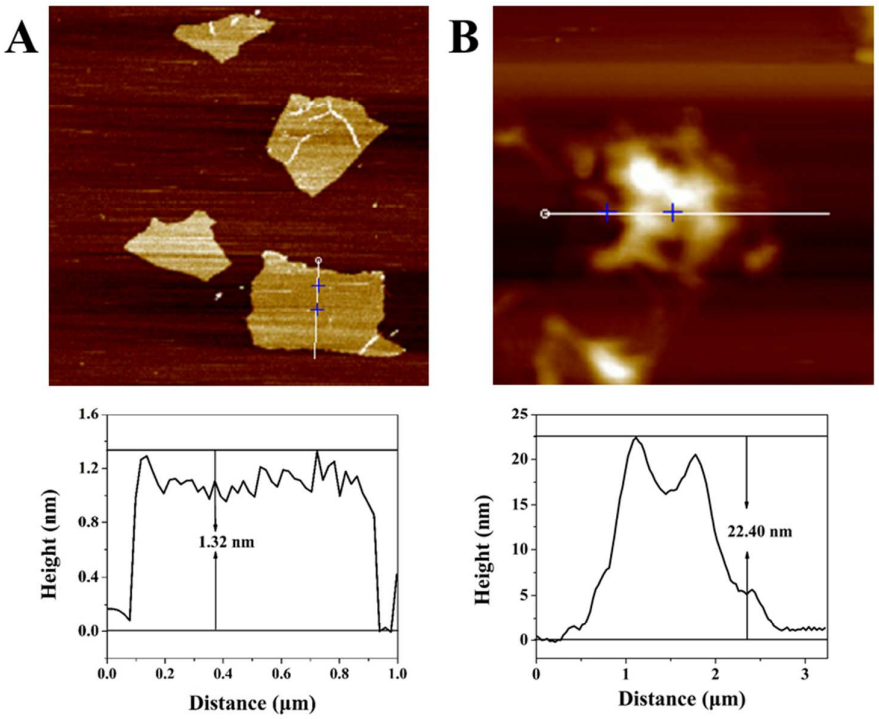

**Figure 1.** AFM images and height profiles of (A) bare GO, (B) probe 1-GO-OTA-aptamer-probe 2-GO on freshly cleaved mica. The height of the naked GO sheets is about 1.32 nm while the formed DNA-mediated GO assembly possessed a thickness of 22.40 nm.

Atomic force microscopy (AFM) was applied to study the structure change during these processes. The height of the naked GO sheets is about 1.32 nm (Figure 1A), which confirms a monolayer state for graphene sheets.[31-32] As displayed in Figure S2, in the absence of GO or $Fe_3O_4$/GO, fluorescent OTA-aptamer (FOTA aptamer) shown a strong fluorescence signal. However, when the GO or $Fe_3O_4$/GO was added to the FOTA aptamer PBS buffer, the fluorescence signal of FOTA aptamer was quenched as a result of ssDNA/GO interaction. Upon mixing the probe 1-GO and probe 2-GO complexes with OTA aptamer, on account of the hybridization of probe 1 and probe 2 with OTA aptamer (as shown in AFM investigations (Figure 1B)), large aggregates can be obtained. The height of slice extracted from the edge of layer from the typical AFM image indicates that the DNA-mediated GO assembly possessed a thickness of 22.40 nm. Obviously, the height data of GO assembly were consistent with the thickness of a multilayers of DNA decorated GO nanosheets.

Preparation and Characterization of GO-labeled Nanoparticles

The detailed preparations and characterizations of $Fe_3O_4$/GO are provided in the supporting information (Figure S1). After obtaining dyes- probe-GO, the PP-probe-GO and MGCB- probe-GO complexes were selected as the examples to illustrate the dye release process. In a basic or acidic environment, PP or MGCB molecules can be effectively released from the GO surfaces and cause color changes respectively. After adding AW (pH 3.0) and then centrifugation, the supernatant color of MGCB-$DNA_3$-GO changed from colorless to dark green. The reason for this phenomenon is that MGCB is converted from a neutral hydrophobic moiety to a cationic hydrophilic moiety[22] and released from the surface of GO. In the UV-vis

spectrum, the color changes correspond to new absorption peaks at 316, 425 and 617 nm, respectively. (Figure S3). It is worth noting that when the order of adding AW and centrifugation is exchanged, there is no color change, which demonstrates a negligible leak of MGCB. In addition, we have optimized the concentration of MGCB, and Figure S5A shows that the optimal MGCB concentration was 2 mM. Besides, a pH of 12.0 for releasing the PP from the GO and the optimized concentration of PP was 2.0 mM after referring to our previous work.[33] We also demonstrated that MV can be released from the surface of GO only at pH 3.0 (Figure S4), and the optimized concentration of TP and MV were 1.5 mM and 2 mM, respectively (Figure S5B and C).

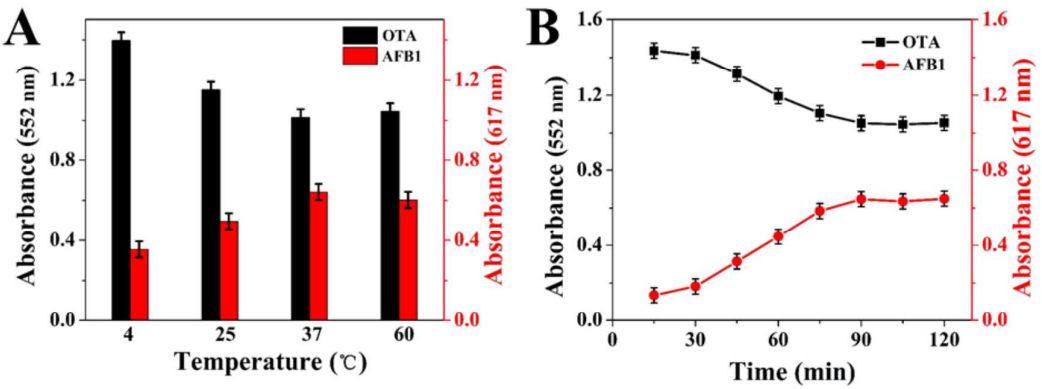


**Figure 2.** The UV–vis absorption spectra responses of the supernatant solution after treating with AW (pH=3.0) and the precipitate solution after treating with BW (pH=12.0) under the different reaction temperature (A) and reaction time (B) with OTA and AFB1 at the concentration of 100 ng $mL^{-1}$. When the temperature was 37℃ and the reaction time was 90 min, the absorption intensity of the supernatant solution reached the maximal value and the absorption intensity of the precipitate solution reached the minimal value.

The optimization of experimental conditions

In order to achieve high accuracy and sensitivity, it is very important to optimize experimental variables involved in whole reaction process. First, the reaction temperature used in the OTA and AFB1 detection was investigated. As shown in

Figure 2A, the UV-vis absorption intensity of the supernatant solution and the precipitate solution were measured at different temperature. When the temperature was 37℃, the maximal value of the UV-vis absorption intensity of the supernatant solution and the minimal value of the UV-vis absorption intensity of the precipitate solution were reached, and then was used as the optimal incubation temperature for the OTA and AFB1 detection. Second, the reaction time of target-aptamer binding was assayed from 10 to 120 min. Figure 2B shows that the UV-vis absorption intensity of the supernatant solution increased and the UV-vis absorption intensity of the precipitate solution decreased at the early stage of the reaction until the time increasing up to 90 min. Beyond the incubation time of 90 min, the absorption intensity reach a plateau. This suggested that 90 min was enough for incubation and the optional incubation time was 90 min in the following detection.

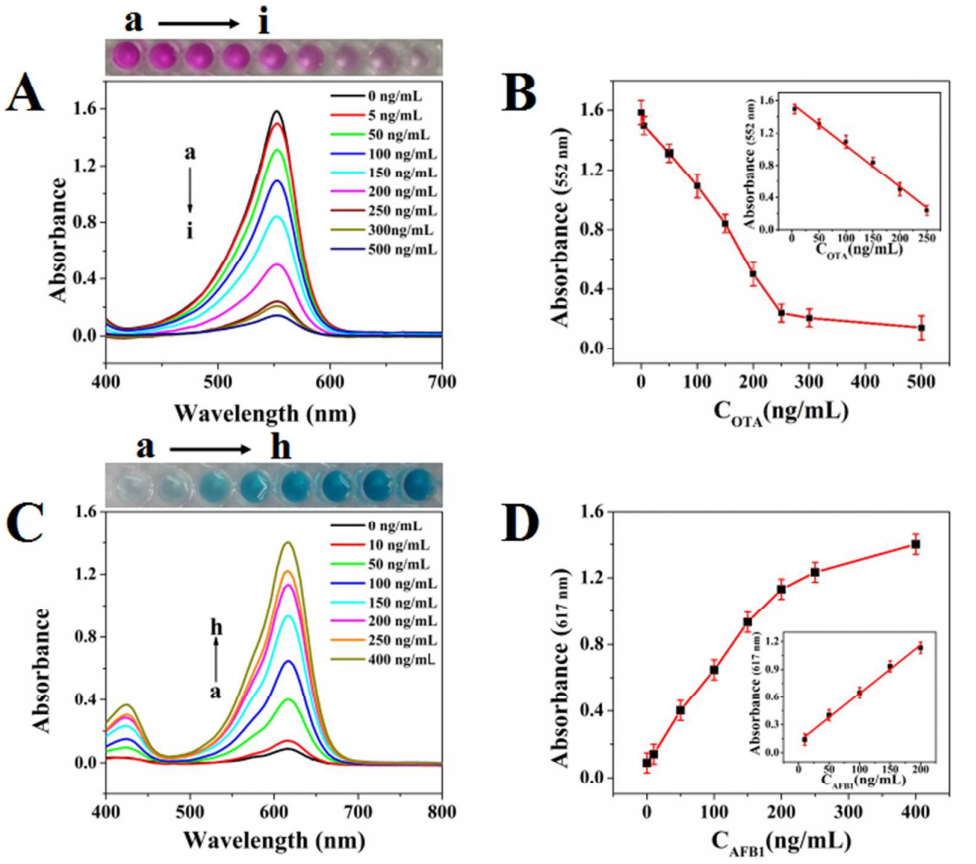

**Figure 3.** (A) The picture and the absorption intensity of the precipitate solution after adding different OTA concentrations (From a to i were 0, 5, 50, 100, 150, 200, 250, 300, 500 ng $mL^{-1}$). (B) The absorption intensity at 552 nm in (A) was plotted as a function of concentration of OTA. The illustration shows the linearity measured at the OTA concentrations range of 5-250 ng $mL^{-1}$. (C) The picture and the absorption intensity of the supernatant solution after adding different AFB1concentrations (From a to h were 0, 10, 50, 100, 150, 200, 250, 400 ng $mL^{-1}$). (D) The absorption intensity at 617 nm in (C) was plotted as a function of concentration of AFB1. The illustration shows the linearity measured at the OTA concentrations range of 10-200 ng $mL^{-1}$.

Simultaneous detection of OTA and AFB1 based on colorimetric biosensor

According to the optimal condition, a rapid, simple, sensitive and feasible colorimetric biosensor for simultaneous multiplex detection was developed. In order to verify the detection performance, OTA and AFB1 were selected as the examples. Different concentrations of OTA and AFB1 were added to the system containing PP-GO-OTA aptamer-$Fe_3O_4$/GO assembly and MGCB-GO-AFB1aptamer-$Fe_3O_4$/GO assembly. As expected, with different concentrations of targets, the color changed and the absorption intensities of the precipitate solution and supernatant solution were shown in Figure 3. The precipitate solution gradually turned from pink to colorless, and as the amount of OTA increased, the intensity of the UV-vis absorption peak at 552 nm gradually decreased (Figure 3A). The supernatant solution gradually turned from colorless to green, the green became more and more deep and the intensity of the UV-vis absorption peak at 617 nm gradually increased with the increase of the amount of AFB1 (Figure 3C). The visible color change could be easily distinguished by naked eyes. Besides, Figure 3B showed a good linear relationship between the intensity of the UV-vis absorption peak of precipitate solution and the concentration of OTA in range of 5-250ng $mL^{-1}$ and Figure 3D also showed the intensity of the UV-vis absorption peak of the supernatant solution and the concentration of AFB1 had a good linear relationship in range of 10-200 ng $mL^{-1}$. In addition, we have summarized the current work and previous methods for the detection of OTA or AFB1 (Table S2). From the reported data and our work in this paper, it can be determined that the

proposed biosensor shows a wide range of linearity and its sensitivity is similar to most other methods.

The selectivity of the colorimetric biosensor

Besides sensitivity, selectivity is another important factor in assessing the performance of the colorimetric biosensor. In order to assess the selectivity of this colorimetric biosensor, control experiments were performed by comparing the sensing results of FB1, OTA, AFB1, AFB1+OTA and OTA+FB1+AFB1. As shown in Figure S6, when the concentration of FB1 was 200 ng $mL^{-1}$, the response singles obtained from FB1 were neglectable.

OTA only affected the absorption peak at wavelength of 552 nm and AFB1 only affected the absorption peak at the wavelength of 617 nm (the concentration of OTA or AFB1 was 100 ng $mL^{-1}$). At the same time, the mixture did not cause a change in absorption compared with the target OTA or AFB1 alone. This result showed that the biosensor had high selectivity.

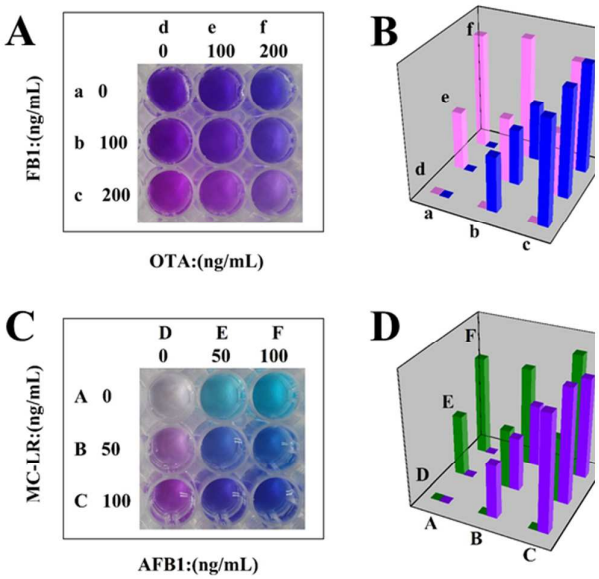


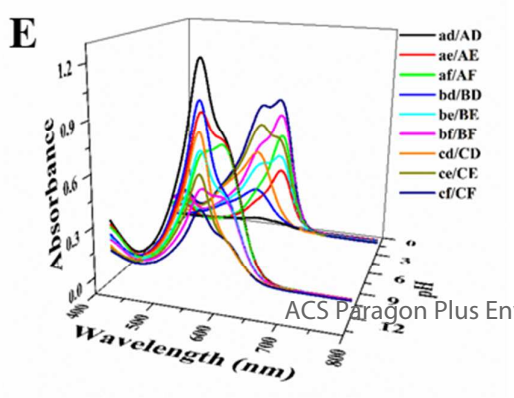


ACS Paragon Plus Environment

**Figure 4.** (A) The picture of supernatant after adding different concentrations of OTA and FB1. (The FB1 concentration from a to c were 0, 100, 200 ng/mL and the OTA concentration from d to f were 0, 100, 200 ng $mL^{-1}$). (B) is the three-dimensional histogram of the OTA and FB1 concentrations achieved by calculating the peak absorption at 552 nm (OTA) and 594 nm (FB1). (C) The picture of supernatant after adding different concentrations of AFB1 and MC-LR. (The AFB1 concentration from A to C were 0, 50, 100 ng/mL and the MC-LR concentration from D to F were 0, 50, 100 ng $mL^{-1}$). (D) is the three-dimensional histogram of the AFB1 and MC-LR concentrations achieved by calculating the peak absorption at 617 nm (AFB1) nm and 570 nm (MC-LR). (E)The UV–vis absorption intensity of the solution after adding different concentrations of OTA and FB1 (pH=12.0), AFB1 and MC-LR (pH=3.0).

Simultaneous detection of four targets based on colorimetric biosensor

When the biosensor was applied for stimultaneous four targets (OTA, FB1, AFB1 and MC-LR) detection. Another two dyes, MV and TP are necessary. Following above principle, after the addition of OTA, AFB1, FB1 and MC-LR, the supernatant solution (acidic condition) and the precipitate solution (alkaline condition) displayed different colors according to the proportion and concentrations of FB1 and OTA (Figure 4A), AFB1 and MC-LR (Figure 4C). And the corresponding UV-vis absorption spectra curves were shown in Figure 4E. It is easy for the naked eye to detect four targets simultaneously and a more accurate result can be achieved by analyzing the peak absorptions in Figure 4E. The concentrations of OTA and FB1 can be calculated with peaks at 552 and 594 nm (Figure 4B) and the concentrations of AFB1 and MC-LR were according to peaks at 570 and 617 nm (Figure 4D). The results agree well with actual concentrations (Table S3).

Real sample analysis

The applicability of the proposed colorimetric biosensor for real sample analysis

was investigated with non-contaminated peanut, the peanut sample was purchased from the local supermarket. The concentrations of OTA and AFB1 in peanut were determined by the standard addition method.[27] The peanut samples were spinked with the mixture of OTA and AFB1 and then detected with the proposed biosensor. The results showed that the recovery rate was 97.82 to 104.29 % (n=3)and the RSD was 3.2-7.2 %, indicating that this biosensor can be applied for OTA and AFB1 detection in actual samples and has a good application prospect in mycotoxin detection (Table 1).

**Table 1** Results of OTA and AFB1 detection in peanuts (n=3).

| Sample | | Added ($ng\ mL^{-1}$) | Found ($ng\ mL^{-1}$) | Recovery (%) | RSD (%) |
|---|---|---|---|---|---|
| 1 | OTA | 5.0 | 5.1 | 102.0 | 5.6 |
| | AFB1 | 10.0 | 10.3 | 103.0 | 3.2 |
| 2 | OTA | 50.0 | 49.4 | 98.8 | 4.8 |
| | AFB1 | 50.0 | 51.9 | 103.8 | 7.2 |
| 3 | OTA | 100.0 | 104.2 | 104.2 | 5.0 |
| | AFB1 | 100.0 | 97.8 | 97.8 | 4.2 |

## Conclusions

In summary, we successfully designed a novel colormetric biosensor for simultaneous four targets detection, demostrating the feasibility of introducing a new dimension to improve the multiplex detection applications of present colormetric detection. With commercially available dyes as signal indicators, the concentrations of targets can be easily obtained in order by adjusting the pH value, which controlled the released of dyes from graphene. Meanwhile, the combination of DNA-directed

self-assembly of graphene oxide and magnetic separation can avoid the complex and expensive chemical modifications processes in the construction of biosensors. And this biosensor showed a good sensitivity and selectivity in peanut samples. The low-cost, universal and simple biosensor can also be used for other targets by using corresponding probes, such as pesticides, illegal additives, heavy metals and so on, which has a great potential for the development of colormetric detection.

## Supporting information

The Supporting Information is available free of charge on the ACS Publications website

Preparation of materials and sensors, characterization of nanomaterials, comparison of the as-prepared methods with those reported in the literatures were provided in supplementary materials.

## Acknowledgments

This work was supported by National Natural Science Foundation of China (Nos. 21505055, 21675066 and 21605055), Natural Science Foundation of Jiangsu Province (No. BK20150486), Special Foundation of China Postdoctoral (2018T110456), China Postdoctoral Science Foundation funded project (2017M621652), Postdoctoral Science Foundation funded project of Jiangsu province (1701075C), Foundation of Jiangsu University (15JDG145), and the Foundation of Key Laboratory of Sensor Analysis of Tumor Marker, Ministry of Education, Qingdao University of Science and Technology (No. SATM201807). Jiangsu Provincial Engineering Laboratory for Advanced Materials of Salt Chemical Industry (No. SF201703) National Key Research and Development Plan (No. 2016YFD0200708).

## REFERENCES

1. Liu, P.; Yang, X.; Sun, S.; Wang, Q.; Wang, K.; Huang, J.; Liu, J.; Li, H. Enzyme-free colorimetric detection of DNA by using Gold Nanoparticles and Hybridization Chain Reaction Amplification. *Analytical Chemistry* ***2013,****85(16), 7689-7695.*

2. Xue, Z.; Yin, B.; Wang, H.; Li, M.; Rao, H.; Liu, X.; Liu, X.; Zhou, X.; Lu, X. An organic indicator functionalized graphene oxide nanocomposite-based colorimetric assay for the detection of sarcosine. *Nanoscale* ***2016,*** *8(10), 5488-5496.*

3. Chen, J.; Jackson, A. A.; Rotello, V. M.; Nugen, S. R. Colorimetric detection of escherichia coli based on the enzyme-induced metallization of Gold Nanorods. *Small* ***2016,*** *12(18), 2469-2475.*

4. Wang, C.; Qian, J.; Wang, K.; Yang, X.; Liu, Q.; Hao, N.; Wang, C.; Dong, X.; Huang, X. Colorimetric aptasensing of ochratoxin A using Au@$Fe_3O_4$ nanoparticles as signal indicator and magnetic separator. *Biosensors & Bioelectronics* **2016,** *77*, 1183-1191.

5. Zhang, S.; Li, H.; Wang, Z.; Liu, J.; Zhang, H.; Wang, B.;Yang, Z. A strongly coupled Au/$Fe_3O_4$/go hybrid material with enhanced nanozyme activity for highly sensitive colorimetric detection, and rapid and efficient removal of Hg(2+) in aqueous solutions. *Nanoscale* ***2015,*** *7(18), 8495-8502.*

6. Yu,Y.; Ying,H.; Peng,G.; Nazeeruddin, M.K. Glutathione modified Gold Nanoparticles for sensitive colorimetric detection of $Pb^{2+}$ ions in rain water polluted

by leaking perovskite solar cells. *Analytical Chemistry* ***2016,*** *88(24), 12316-12322.*

7. Pittet, A.; Royer, D. Rapid, low cost thin-layer chromatographic screening method for the detection of ochratoxin A in green coffee at a control level of 10 mu g/kg. *Journal of Agricultural and Food Chemistry* **2002,** *50* (2), 243-247.

8. Thomas, K.; Wechsler, D.; Chen, Y.-M.; Crain, S.; Quilliam, M. A. Analysis of natural toxins by liquid chromatography-chemiluminescence nitrogen detection and application to the preparation of certified reference materials. *Journal of Aoac International* **2016,** *99* (5), 1173-1184.

9. Barber, J. Photosynthetic energy conversion: natural and artificial. *chem soc rev* ***2009,*** *38(1), 185-196.*

10. Liu, Y.; Yuan, M.; Qiao, L.; Guo, R. An efficient colorimetric biosensor for glucose based on peroxidase-like protein-Fe3O4, and glucose oxidase nanocomposites. *Biosensors & Bioelectronics* ***2014,****52(52C), 391-396.*

11. Zhang, S.; Zhang, Z.; Wang, T.; Zhang, D.; Li, X.; Xue, Z.; Shan, D.; Lu, X. High-throughput and ultratrace naked-eye colorimetric detection of Au(3+) based on the Gold amalgam-stimulated peroxidase mimetic activity in aqueous solutions. *Chemical Communications* ***2017,*** *53(36), 5056-5058.*

12. Cai, S.; Han, Q.; Qi, C.; Lian, Z.; Jia, X.; Yang, R.; Wang, C. $Pt_{74}Ag_{26}$ nanoparticle-decorated ultrathin $MoS_2$ nanosheets as novel peroxidase mimics for highly selective colorimetric detection of $H_2O_2$ and glucose. *Nanoscale* ***2016,*** *8(6), 3685-3693.*

13. Liu, Q.; Yang, Y.; Li, H.; Zhu, R.; Shao, Q.; Yang, S.; Xu, J. NiO nanoparticles

modified with 5,10,15,20-tetrakis(4-carboxyl pheyl)-porphyrin: promising peroxidase mimetics for $H_2O_2$ and glucose detection. *Biosensors & bioelectronics* ***2015****, 64, 147-153.*

14. Liu, H.; Ding, Y.; Yang, B.; Liu, Z.; Liu, Q.; Zhang, X. Colorimetric and ultrasensitive detection of $H_2O_2$ based on Au/$Co_3O_4$-CeOx nanocomposites with enhanced peroxidase-like performance. *Sensors and Actuators B: Chemical* ***2018****, 271, 336-345.*

15. Li, X.; Wu, Z.; Zhou, X.; Hu, J. Colorimetric response of peptide modified Gold Nanoparticles: an original assay for ultrasensitive Silver detection. *Biosensors & Bioelectronics* ***2016,*** *92, 496-501.*

16. Zhang, Z.; Chen, Z.; Qu, C.; Chen, L. Highly Sensitive Visual Detection of Copper Ions Based on the Shape-Dependent LSPR Spectroscopy of Gold Nanorods. *Langmuir the Acs Journal of Surfaces & Colloids* ***2014,*** *30(12), 3625-3630.*

17. Ma, X.; Chen, Z.; Kannan, P.; Lin, Z.; Qiu, B.; Guo, L. Gold Nanorods as colorful chromogenic substrates for semiquantitative detection of nucleic acids, proteins, and small molecules with the naked eye. *Analytical Chemistry* **2016,** *88* (6), 3227-3234.

18. Mcvey, C.; Huang, F.; Elliott, C.; Cao, C. Endonuclease controlled aggregation of Gold Nanoparticles for the ultrasensitive detection of pathogenic bacterial DNA. *Biosensors & Bioelectronics* ***2017,*** *92, 502-508.*

19. Gopinath, S. C.; Lakshmipriya, T.; Awazu, K. Colorimetric detection of

controlled assembly and disassembly of aptamers on unmodified Gold Nanoparticles. *Biosensors & Bioelectronics* ***2014,*** *51(3), 115-123.*

20. Ren, X.; Yan, J.; Wu, D.; Wei, Q.; Wan, Y. Nanobody-Based Apolipoprotein E Immunosensor for Point-of-Care Testing. *ACS sensors* ***2017****, 2 (9), 1267-1271.*

21. Mancuso, M.; Jiang, L.; Cesarman, E.; Erickson, D. Multiplexed colorimetric detection of Kaposi's sarcoma associated herpesvirus and Bartonella DNA using Gold and Silver Nanoparticles. *Nanoscale* ***2013,*** *5 (4), 1678-1686*.

22. Li, C.; Yang, Y.; Wu, D.; Li, T.; Yin, Y.; Li, G. Improvement of enzyme-linked immunosorbent assay for the multicolor detection of biomarkers. *Chemical Science* **2016***, 7 (5), 3011-3016.*

23. Han, Q.; Wang, R.; Xing, B.; Chi, H.; Wu, D.; Wei, Q. Label-free photoelectrochemical aptasensor for tetracycline detection based on cerium doped CdS sensitized $BiYWO_6$. *Biosensors & bioelectronics* ***2018****, 106, 7-13.*

24. Xing, B.; Zhu, W.; Zheng, X.; Zhu, Y.; Wei, Q.; Wu, D. Electrochemiluminescence immunosensor based on quenching effect of $SiO_2$ @PDA on $SnO_2$ /rGO/Au NPs-luminol for insulin detection. *Sensors and Actuators B: Chemical* ***2018****, 265, 403-411.*

25. Hussein, H.S.; Brasel, J.M. Toxicity, metabolism, and impact of mycotoxins on humans and animals. *Toxicology* ***2001,*** *167, 101–134.*

26. Liu, L. H.; Zhou, X. H.; Shi, H. C. Portable optical aptasensor for rapid detection of mycotoxin with a reversible ligand-grafted biosensing surface. *Biosensors & Bioelectronics* ***2015,*** *72, 300-305.*

27. Zhou, Z.; Hao, N.; Zhang, Y.; Hua, R.; Qian, J.; Liu, Q.; Li, H.; Zhu, W.; Wang, K. A novel universal colorimetric sensor for simultaneous dual target detection through DNA-directed self-assembly of graphene oxide and magnetic separation. *Chemical Communications* ***2017,*** *53 (52), 7096-7099.*

28. Ren, X.; Zhang, T.; Wu, D.; Yan, T.; Pang, X.; Du, B.; Lou, W.; Wei, Q. Increased electrocatalyzed performance through high content potassium doped graphene matrix and aptamer tri infinite amplification labels strategy: Highly sensitive for matrix metalloproteinases-2 detection. *Biosensors & bioelectronics* **2017,** *94*, 694-700.

29. Ren, X.; Ma, H.; Zhang, T.; Zhang, Y.; Yan, T.; Du, B.; Wei, Q. Sulfur-Doped Graphene-Based Immunological Biosensing Platform for Multianalysis of Cancer Biomarkers. *ACS applied materials& interfaces* **2017,** *9* (43), 37637-37644.

30. Yang, L.; Li, Y.; Zhang, Y.; Fan, D.; Pang, X.; Wei, Q.; Du, B. 3D Nanostructured Palladium-Functionalized Graphene-Aerogel-Supported $Fe_3O_4$ for Enhanced $Ru(bpy)_3(2+)$-Based Electrochemiluminescent Immunosensing of Prostate Specific Antigen. *ACS applied materials & interfaces* **2017,** *9* (40), 35260-35267.

31. Xiao, F.; Song, J.; Gao, H.; Zan, X.; Xu, R.; Duan, H. Coating graphene paper with 2D-Assembly of electrocatalytic nanoparticles: A modular approach toward High-Performance Flexible Electrodes. *ACS Nano* ***2012,*** *6 (1), 100-110.*

32. Stankovich, S.; Piner, R. D.; Nguyen, S. T.; Ruoff, R. S. Synthesis and exfoliation of isocyanate-treated graphene oxide nanoplatelets. *Carbon* ***2006,*** *44 (15), 3342-3347.*

33. Wang, B.; Wu, Y.; Chen, Y.; Weng, B.; Xu, L.; Li, C. A highly sensitive

aptasensor for OTA detection based on hybridization chain reaction and fluorescent perylene probe. *Biosensors & Bioelectronics* ***2016,*** *81, 125-130.*

For TOC only

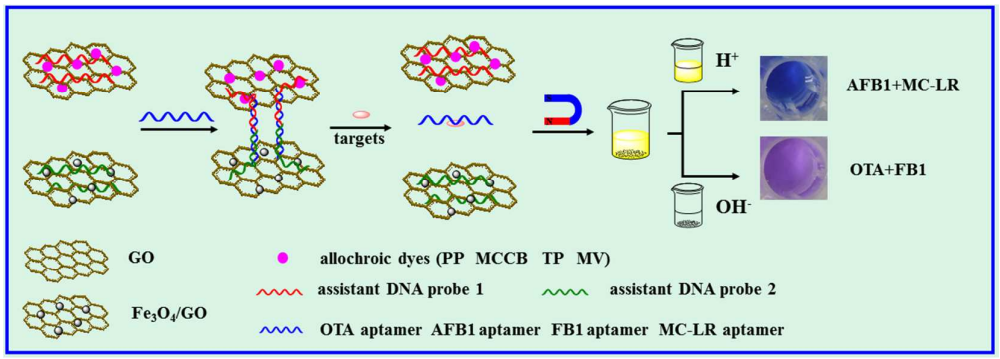


A colorimetric biosensor based on the DNA-mediated GO assembly was developed for OTA, AFB1, FB1, MC-LR detection. After the biorecognition and magnetic separation, pH value was introduced as the new dimension to control the release order of dyes from the graphene to quantify targets